

Supplementary Information

Insight into the reactivity of in-situ formed $\{(\text{NbO}_2)_3\text{SiW}_9\}$: synthesis, structure, and solution properties of a trimeric polytungstosilicate trapping a $\{\text{MnNb}_9\}$ core

Haiying Wang, Zhijie Liang, Yaya Wang, Dongdi Zhang*, Pengtao Ma, Jingping Wang and Jingyang Niu*

Henan Key Laboratory of Polyoxometalate Chemistry, Institute of Molecular and Crystal Engineering
College of Chemistry and Chemical Engineering, Henan University, Kaifeng, 475004 Henan, China

CONTENTS

1. Table S1. The reported $\{\text{Nb}_3\text{SiW}_9\}$ -based POMs.
2. Table S2. Bond valence sum (BVS) calculations for Mn center in **1**.
3. Figure S1. XPS spectrum for **1a**.
4. Table S3. BVS results of all the atoms in **1**.
5. Figure S2. Representation of the $\{\text{Mn}^{\text{II}}\text{O}_3(\text{H}_2\text{O})_3\}$ core in **1**.
6. Figure S3. IR spectra of **1a**, SiW_9 and $\{(\text{NbO}_2)_3\text{SiW}_9\}$
7. Figure S4. Cyclic voltammetry (CV) studies of **1a** and SiW_9
8. Figure S5. UV-vis spectra of **1a**, SiW_9 and $\{(\text{NbO}_2)_3\text{SiW}_9\}$
9. Figure S6. TG-MS curves of **1a**
10. Figure S7. The comparison of experimental XRPD patterns (blue) and simulated (black) of **1a**

Table S1. The reported {Nb₃SiW₉}-based POMs.

Polyanion	oligomeric	Ref	Journal name
{XW ₉ (NbO ₂) ₃ O ₃₇ } X= Si, Ge, P, As	1	Hill et al. (2003) /	Bull. Korean Chem. Soc./
		Liu et al. (2010) /	Chem. Eur. J. /
		Hill et al. (1998) /	Inorg. Chem. /
		Liu et al. (2011)	Inorg. Chim. Acta.
{XW ₉ Nb ₃ O ₄₀ } X= Si, Ge, P, As	1	Finke et al. (1984) /	J. Am. Chem. Soc. /
		Liu et al. (2010) /	Chem. Eur. J. /
		Liu et al. (2011) /	Inorg. Chem. /
[SiW ₁₁ (NbO ₂)O ₃₉] ⁵⁻	1	Hill et al. (1994)	J. Med. Chem.
[PW ₁₁ NbO ₄₀] ⁷⁻	1	Radkov et al. (1995)	Polyhedron
[P ₂ W ₁₇ (NbO ₂)O ₆₁] ⁷⁻	1	Hill et al. (2001)	J. Am. Chem. Soc.
[P ₂ W ₁₇ NbO ₆₂] ⁷⁻	1	Hill et al. (2001)	J. Am. Chem. Soc.
[P ₂ W ₁₂ (NbO ₂) ₆ O ₅₆] ¹²⁻	1	Hill et al. (1997)	J. Am. Chem. Soc.
[P ₂ W ₁₅ Nb ₃ O ₆₂] ⁹⁻	1	Finke et al. (1988) / (2014)	Organometallics/ Inorg. Chem.
[Ln ₆ (H ₂ O) ₃₈ [P ₂ W ₁₅ Nb ₃ O ₆₂] ₄] ¹⁸⁻ (Ln = Ce ³⁺ , Eu ³⁺)	1	Liu et al. (2012)	Eur. J. Inorg. Chem.
[(Si ₂ W ₁₈ Nb ₆ O ₇₈)Cr(H ₂ O) ₄] ⁷⁻	2	Su et al. (2013)	ChemPlusChem.
[(Si ₂ W ₁₈ Nb ₆ O ₇₈)Cr ₂ (H ₂ O) ₈] ⁴⁻			
[(Si ₂ W ₁₈ Nb ₆ O ₇₈)FeCl ₂ (H ₂ O) ₂] ⁹⁻			
[Si ₂ W ₁₈ Nb ₆ O ₇₇] ⁸⁻	2	Finke et al. (1984)/ Hill et al. (1999)	J. Am. Chem. Soc./ Chem. Commun.
[Si ₂ W ₁₈ Nb ₆ O ₇₈] ¹⁰⁻	2	Hill et al. (2003)	Inorg. Chem.
[Nb ₂ K(H ₂ O) ₄ (A-α-SiW ₉ O ₃₄) ₂] ⁹⁻	2	Niu et al. (2012)	Inorg. Chem. Commun.
[(Ge ₂ W ₁₈ Nb ₆ O ₇₈)Eu(H ₂ O) ₄] ⁷⁻	2	Liu et al. (2012)	CrystEngComm.
[H ₁₅ Ge ₂ W ₁₈ Nb ₈ O ₈₈] ⁵⁻	2	Liu et al. (2010)	Chem. Eur. J.
[{P ₂ W ₁₂ Nb ₄ O ₅₉ (NbO ₂) ₂] ₂] ²⁰⁻	2	Yue et al. (2014)	Inorg. Chem. Commun.
[{P ₂ W ₁₂ Nb ₆ (O ₂) ₄ O ₅₇] ₂] ²⁰⁻	2	Niu et al. (2015)	Inorg. Chem. Front.
[{P ₂ W ₁₂ Nb ₇ O ₆₃ (H ₂ O) ₂] ₄ {Nb ₄ O ₄ (OH) ₆] ₃] ³⁰⁻	4	Niu et al. (2015)	Inorg. Chem. Front.
[{Nb ₄ O ₆ (OH) ₄ }{Nb ₆ P ₂ W ₁₂ O ₆₁ }] ₄] ³⁶⁻	4	Niu et al. (2014)	Inorg. Chem.
[Nb ₄ O ₆ (Nb ₃ SiW ₉ O ₄₀) ₄] ²⁰⁻	4	Hill et al. (1999)/ Su et al. (2014)	Angew. Chem., Int. Ed. / Inorg. Chem. Commun.
[(Ge ₄ W ₃₆ Nb ₁₂ O ₁₅₆)Eu(H ₂ O) ₃] ¹⁷⁻	4	Liu et al. (2012)	CrystEngComm.
[Cs(GeW ₉ Nb ₃ O ₄₀) ₄ (SO ₄)Eu ₅ (H ₂ O) ₃₆] ¹⁴⁻	4	Liu et al. (2012)	CrystEngComm.
[Cs ₂ (GeW ₉ Nb ₃ O ₄₀) ₄ Eu ₄ (H ₂ O) ₂₂] ¹⁴⁻	4	Liu et al. (2012)	CrystEngComm.
[Ge ₄ W ₃₆ Nb ₁₆ O ₁₆₆] ²⁰⁻	4	Liu et al. (2010)	Chem. Eur. J.
[{Nb ₄ O ₆ (OH) ₄ }{Nb ₆ P ₂ W ₁₂ O ₆₁ }] ₄] ³⁶⁻	4	Niu et al. (2014)	Inorg. Chem.
[Nb ₄ O ₆ (Nb ₃ AsW ₉ O ₄₀) ₄] ¹⁶⁻	4	Liu et al. (2011)	Inorg. Chim. Acta.
{Mn ₁₅ (Nb ₆ P ₂ W ₁₂ O ₆₂) ₆ }	6	Niu et al. (2015)	Chem. Eur. J.

$[(\text{GeW}_9\text{Nb}_3\text{O}_{40})_4\text{Eu}_{5.5}(\text{H}_2\text{O})_{26}]^{11.5-}$	1D	Liu et al. (2012)	CrystEngComm.
$[\text{GeW}_9\text{Nb}_3\text{O}_{40}\text{Eu}_{1.25}(\text{H}_2\text{O})_{12}]^{3.25-}$	2D	Liu et al. (2012)	CrystEngComm.

Table S2. Bond valence sum (BVS) values for the Mn center in 1. The assigned oxidation states are highlighted in yellow background.

	BVS value		
	Mn(II)	Mn(III)	Mn(IV)
Mn	2.45	2.06	2.26

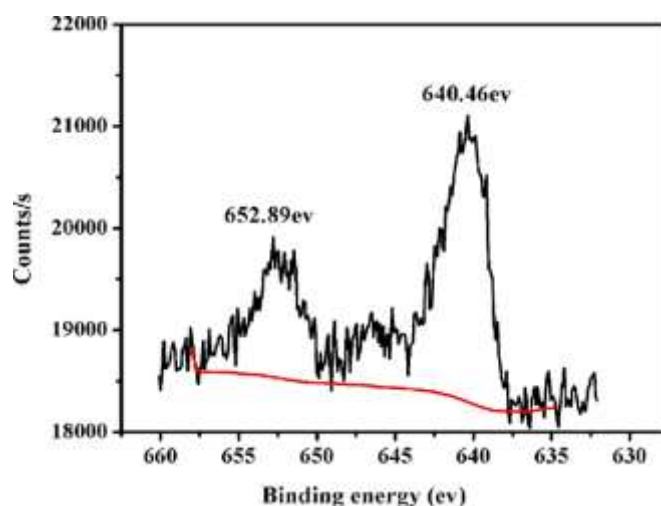


Figure S1. XPS spectrum for 1a. (The red line represents the baseline)

Table S3. BVS calculation results of all the atoms on polyanion 1. Because the BVS value of O1W is 0.38, which is less than 0.5 and can be commonly considered to be deprotonated. Therefore, it is shown in red to highlight this.

Atom Code	Bond Valence	Atom Code	Bond Valence	Atom Code	Bond Valence
Si1	3.95	O4	1.82	O15	1.95
Nb1	4.87	O5	1.89	O16	2.00
Nb2	4.80	O6	2.09	O17	1.53
W1	5.94	O7	1.99	O18	1.82
W2	5.85	O8	1.94	O19	1.93
W3	5.88	O9	1.98	O20	1.73
W4	6.28	O10	1.52	O21	1.99

W5	5.93	O11	2.02	O22	1.62
O1	1.82	O12	1.84	O23	1.88
O2	2.08	O13	1.96	O24	2.04
O3	1.79	O14	1.59	O1W	0.38

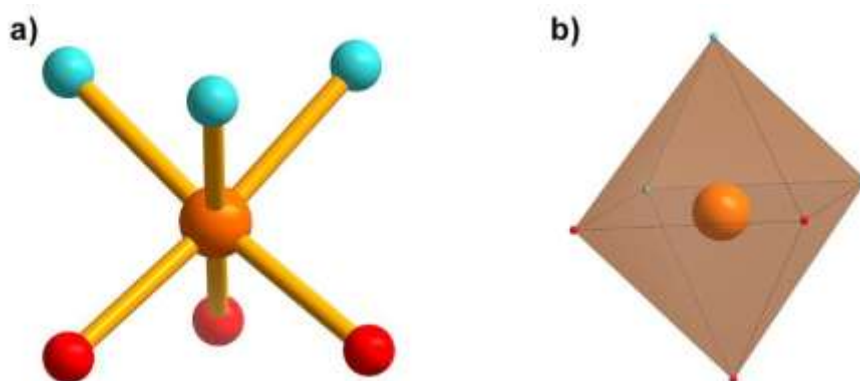


Figure S2. a) Representation of the $\{\text{Mn}^{\text{II}}\text{O}_3(\text{H}_2\text{O})_3\}$ core in **1** highlighting the di-protonated oxygens; b) the coordination geometric framework of the Mn ion. Mn: orange, O: red, H₂O: aqua.

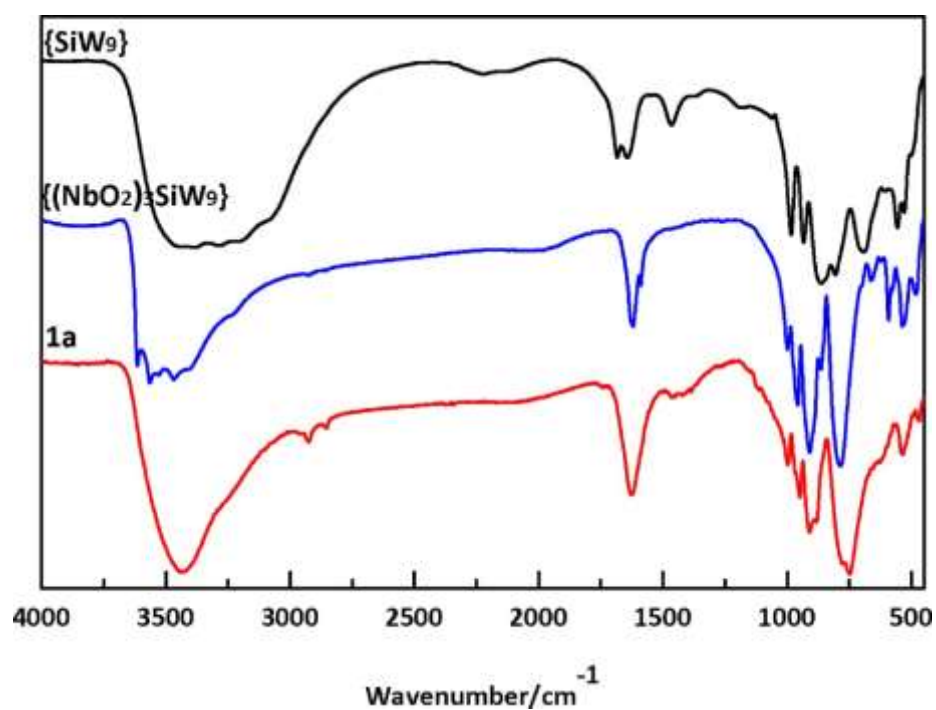


Figure S3. IR spectra of **1a**, SiW₉ and {(NbO₂)₃SiW₉} in the region between 4000 to 450 cm⁻¹.

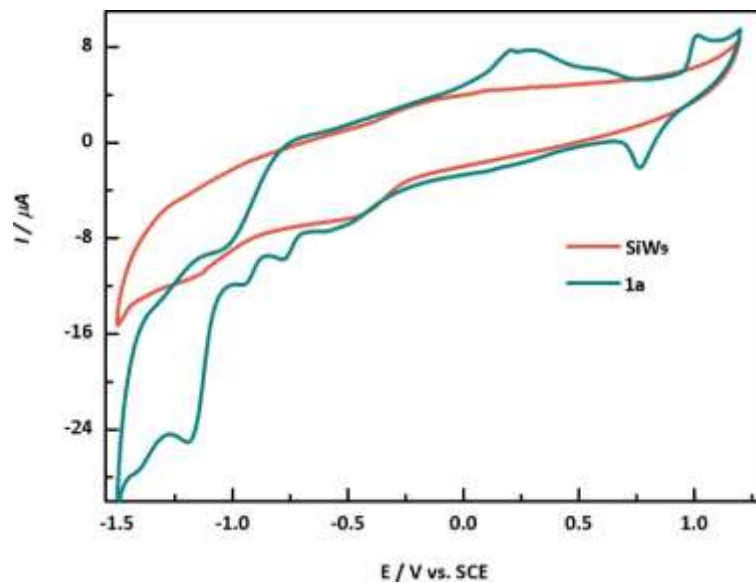


Figure S4. Cyclic voltammetry (CV) studies of 2×10^{-4} M polyanion 1a and SiW_9 in a pH 4 medium ($0.5 \text{ M Na}_2\text{SO}_4$).

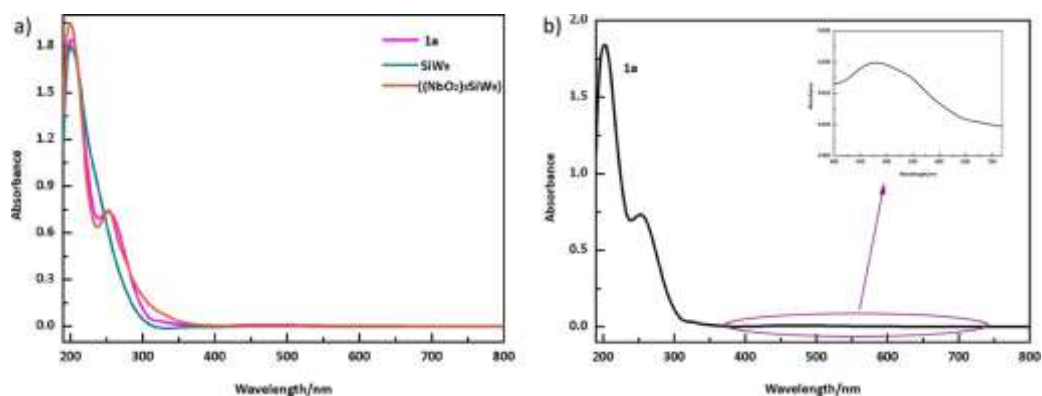


Figure S5. a) The UV spectra of 1a, SiW_9 and $\{(\text{NbO}_2)_3\text{SiW}_9\}$ in the region of 800–200 nm. b) The highlight of the weak absorption band at 478nm in the visible region resulting from the d–d electron transition of Mn^{II} . The inset figure is the enlarged drawing in the region of 400-700 nm in different coordinates.

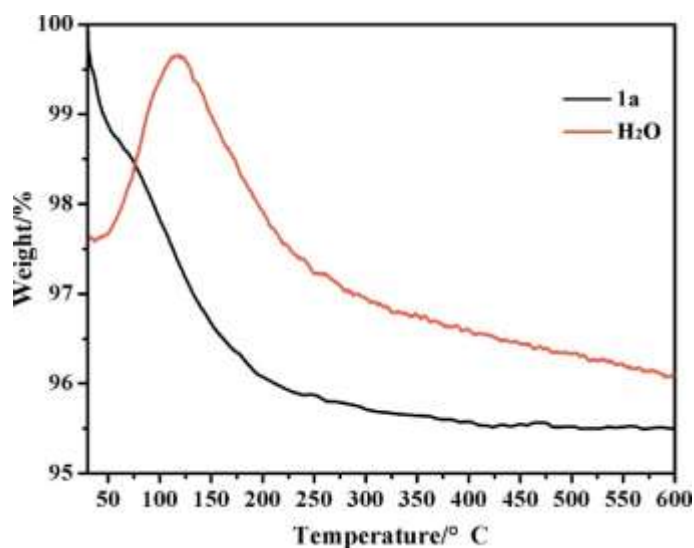


Figure S6. TG-MS curve of 1a. Black line: the TG curves. Red line: the relative content of water during the test process. Pyrolysis experiment of 1a was investigated under nitrogen atmosphere by thermogravimetric-mass spectrometry (TG-MS), which can identify the possible products during the thermolysis process. As shown in Fig. S6, the weight loss in the range of 0–380 °C could be attributed to the loss of water molecules. The orange curve represents the product of water tested by mass spectrometry during the heating process.

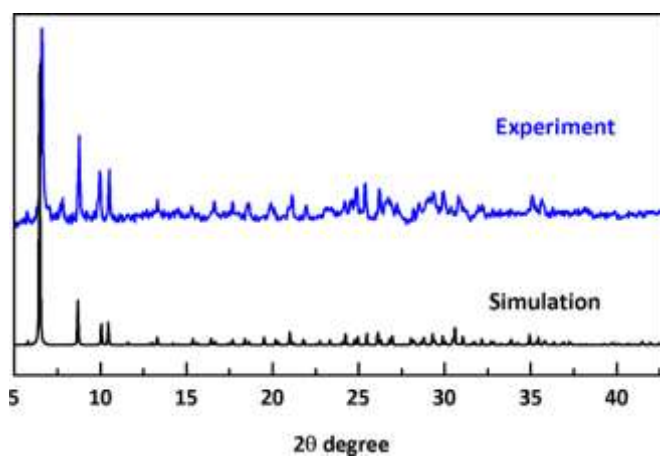


Figure S7. The comparison of experimental (blue) and simulated (black) XRPD patterns of 1a.